A parameter identification technique for traffic speed deflectometer tests of pavements

Sun, Zhaojie; Kasbergen, Cor; van Dalen, Karel N.; Anupam, Kumar; Skarpas, Athanasios; Erkens, Sandra M.J.G.

DOI
10.1080/14680629.2022.2060125

Publication date
2022

Document Version
Final published version

Published in
Road Materials and Pavement Design

Citation (APA)
Sun, Z., Kasbergen, C., van Dalen, K. N., Anupam, K., Skarpas, A., & Erkens, S. M. J. G. (2022). A parameter identification technique for traffic speed deflectometer tests of pavements. *Road Materials and Pavement Design*, *24*(4), 1065-1087. https://doi.org/10.1080/14680629.2022.2060125

Road Materials and Pavement Design

ISSN: (Print) (Online) Journal homepage: https://www.tandfonline.com/loi/trmp20

A parameter identification technique for traffic speed deflectometer tests of pavements

Zhaojie Sun, Cor Kasbergen, Karel N. van Dalen, Kumar Anupam, Athanasios Skarpas & Sandra M. J. G. Erkens

To cite this article: Zhaojie Sun, Cor Kasbergen, Karel N. van Dalen, Kumar Anupam, Athanasios Skarpas & Sandra M. J. G. Erkens (2022): A parameter identification technique for traffic speed deflectometer tests of pavements, Road Materials and Pavement Design, DOI: 10.1080/14680629.2022.2060125

To link to this article: https://doi.org/10.1080/14680629.2022.2060125

Published online: 20 Apr 2022.

ROAD MATERIALS AND PAVEMENT DESIGN
https://doi.org/10.1080/14680629.2022.2060125

Taylor & Francis
Taylor & Francis Group

A parameter identification technique for traffic speed deflectometer tests of pavements

Zhaojie Sun [a], Cor Kasbergen [a], Karel N. van Dalen [a], Kumar Anupam [a], Athanasios Skarpas [a,b] and Sandra M. J. G. Erkens [a]

[a]Department of Engineering Structures, Faculty of Civil Engineering and Geosciences, Delft University of Technology, Delft, The Netherlands; [b]Department of Civil Infrastructure and Environmental Engineering, College of Engineering, Khalifa University, Abu Dhabi, United Arab Emirates

ABSTRACT

The structural evaluation of existing pavements forms the basis for formulating cost-effective maintenance and rehabilitation strategies. A promising tool for pavement structural evaluation at network level is the Traffic Speed Deflectometer (TSD) test. However, the application of the TSD test is hindered by the lack of a robust and efficient parameter identification technique. To solve this problem, a theoretical model for the TSD test is first formulated. Then, a minimisation algorithm which works best with the theoretical TSD model for parameter identification is selected. Finally, the performance of this combination in processing field TSD measurements is studied. The results show that the modified Levenberg-Marquardt algorithm using all the 9 detection points is most suitable to be combined with the theoretical TSD model for parameter identification, which gives a promising parameter identification technique for TSD tests of pavements. The presented work contributes to the development of technologies for pavement structural evaluation.

ARTICLE HISTORY
Received 23 May 2021
Accepted 26 March 2022

KEYWORDS
Pavement; Moving load; Parameter identification technique; Traffic Speed Deflectometer; Minimisation algorithm

1. Introduction

The development of roadway networks improves the convenience of life, while the inevitable deterioration of existing pavements reduces the comfort and safety of users. In order to maintain and recover the service performance of pavements, proper maintenance and rehabilitation activities are needed. The desired maintenance and rehabilitation strategies should be cost-effective enough to ensure that appropriate treatments are applied on necessary pavement sections at the right time. The formulation of these strategies depends on the structural performance of existing pavements, which can be evaluated by structural analysis if corresponding structural parameters are known. The important structural parameters for pavement structural analysis are layer moduli and layer thicknesses, which can be elegantly predicted by a so-called parameter identification technique based on non-destructive testing results of pavements. The desired parameter identification technique should be not only numerically robust to obtain accurate results, but also computationally efficient to be suitable for practical application (Al-Khoury et al., 2001a; Al-Khoury et al., 2001b; Lee et al., 2019). The most important component of a parameter identification technique is a theoretical model which can predict the response of pavements caused by certain loads. On the basis of the theoretical model, an iterative,

CONTACT Zhaojie Sun zhaojie.sun@tudelft.nl
This article has been republished with minor changes. These changes do not impact the academic content of the article.

statistical, or genetic technique can be developed to identify parameters of pavements by analysing corresponding response (Lee et al., 2017; Nielsen, 2019; Sun et al., 2020a).

Non-destructive testing methods are widely used for pavement structural evaluation because they are time-saving and structure-friendly (Maser, 2003). The most commonly used non-destructive testing method in the field of pavement engineering is the Falling Weight Deflectometer (FWD) test, which measures the time-dependent pavement response caused by an impact load (Kutay et al., 2011). The FWD test of pavements can be properly simulated by a theoretical model considering wave propagation, which can be further combined with a nonlinear minimisation algorithm to achieve parameter identification based on FWD measurements. However, the low mobility of the FWD test makes it not that suitable for pavement structural evaluation at network level (Sun et al., 2020b). To solve this issue, some non-destructive testing methods with high mobility have been developed, such as the Traffic Speed Deflectometer (TSD) test.

The TSD device has a similar appearance to a truck trailer and it can measure the slopes of vertical deflection at a set of points along the midline of the right rear wheel pair on the pavement surface at normal driving speeds. Because of this feature, the TSD test is very suitable for network-level pavement structural evaluation. Some studies had investigated the methods of using TSD measurements for pavement structural evaluation. For example, Nasimifar et al. (2019) developed a practical approach to compute the effective structural number (SN_{eff}) of in-service flexible pavements from TSD measurements; the computed SN_{eff} can be used for network-level pavement structural evaluation. Katicha et al. (2014) used a wavelet-transform denoising technique to obtain TSD deflection slope measurements without noises, the use of which gives improved pavement structural evaluation. Zihan et al. (2019) investigated the relationship between surface indices (e.g. the random cracking index, the roughness index, the rutting index, etc.) and in-service pavement structural conditions predicted from traffic speed deflection devices to assess the feasibility of identifying structurally damaged sections by only using surface indices or their declining rates.

However, the number of studies on the application of TSD measurements for identifying structural parameters of pavements is very limited. For example, Nasimifar et al. (2017) proposed a technique that can identify the elastic and viscoelastic layer moduli of asphalt pavements from TSD measurements via a trial-and-error process; this technique uses a software called 3D-Move as the computational kernel. Furthermore, Liu et al. (2018) developed a parameter identification technique by combining a semi-analytical finite element model with the Artificial Neural Network (ANN) algorithm; this technique can identify the elastic layer moduli of asphalt pavements by analysing corresponding TSD measurements. In addition, Wu et al. (2020) formulated a parameter identification technique based on a 2.5D finite element model and the constrained extended Kalman filter (CEKF) to determine the elastic layer moduli of pavements by analysing the response caused by moving loads. However, these techniques are still not good enough to be used for network-level pavement structural evaluation. To address this issue, a robust and efficient parameter identification technique for TSD tests of pavements will be developed in this study by combining a novel theoretical TSD model and an appropriate minimisation algorithm. The work presented in this paper contributes to the development of technologies for pavement structural evaluation.

2. A theoretical model for the TSD test

In this section, a theoretical model for the TSD test of pavements is formulated. Based on this model, the characteristics and parameter sensitivity of the response of pavements caused by the TSD loading are investigated.

2.1. Model formulation and solution scheme

As shown in Figure 1, the TSD test of pavements is theoretically modelled by a layered system subjected to surface moving loads. Each layer of the layered system is a well-defined continuum and all

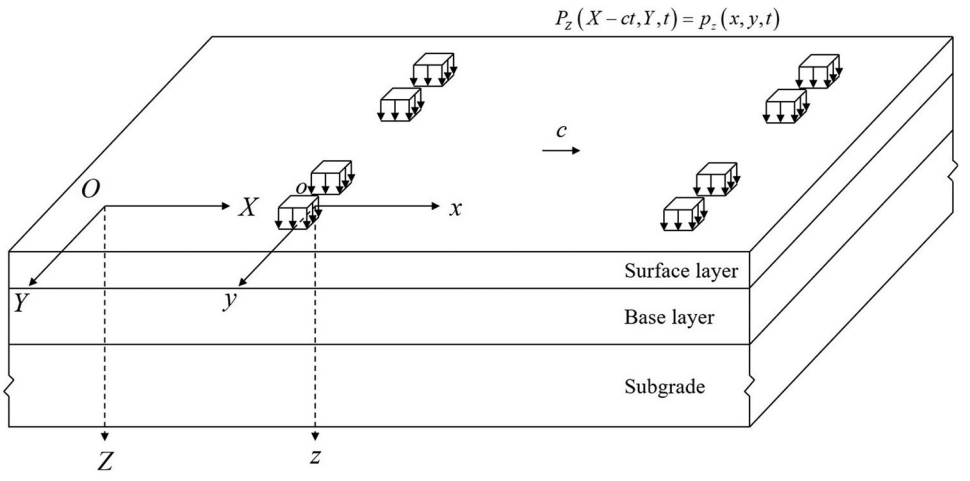

Figure 1. Schematic representation of the TSD test of pavements.

the layers are fully bonded. In practice, the TSD device always measures the response of points around the load, so it is convenient to introduce both a stationary Cartesian coordinate system (*OXYZ*) and a moving Cartesian coordinate system (*oxyz*). The stationary coordinate system is stationary and its origin is located in the centre of the initial loading area of the right rear wheel pair of the TSD device, while the moving coordinate system is moving with the load and its origin is located in the centre of the moving loading area of the right rear wheel pair. These two coordinate systems are coincident when the time t is zero. The load is assumed to be moving in the positive X-direction with a constant speed c, which results in the following coordinate relationships (Sun et al., 2022):

$$x = X - ct, \quad y = Y, \quad z = Z \tag{1}$$

Moreover, the partial derivatives in the two coordinate systems have the following relationships for nonnegative integer n:

$$\partial_X^n = \partial_x^n, \quad \partial_Y^n = \partial_y^n, \quad \partial_Z^n = \partial_z^n \tag{2}$$

$$\partial_t^n|_{OXYZ} = (\partial_t - c\partial_x)^n|_{oxyz} \tag{3}$$

where ∂_X^n means the n-th order derivative with respect to X, the subscripts '*OXYZ*' and '*oxyz*' mean that corresponding quantities are expressed in the stationary coordinate system and the moving coordinate system, respectively. In addition, the following Fourier transform pair is used in this study to transform quantities in the space–time domain to their counterparts in the wavenumber-frequency domain:

$$\tilde{q}(k_x, k_y, z, \omega) = \int_{-\infty}^{\infty}\int_{-\infty}^{\infty}\int_{-\infty}^{\infty} q(x, y, z, t) e^{\mathrm{i}(k_x x + k_y y - \omega t)} dx dy dt \tag{4}$$

$$q(x, y, z, t) = \frac{1}{(2\pi)^3}\int_{-\infty}^{\infty}\int_{-\infty}^{\infty}\int_{-\infty}^{\infty} \tilde{q}(k_x, k_y, z, \omega) e^{-\mathrm{i}(k_x x + k_y y - \omega t)} dk_x dk_y d\omega \tag{5}$$

in which i is the imaginary unit satisfying $\mathrm{i}^2 = -1$, k_x is the wavenumber in the x-direction, k_y is the wavenumber in the y-direction, ω is the angular frequency, $q(x, y, z, t)$ is an arbitrary quantity in the space–time domain, and $\tilde{q}(k_x, k_y, z, \omega)$ is the counterpart of this quantity in the wavenumber-frequency domain.

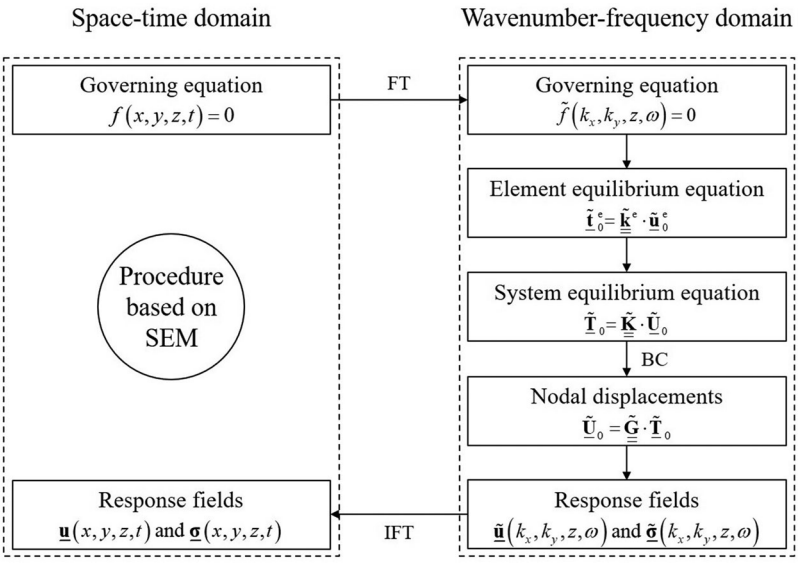

Figure 2. The SEM-based procedure to calculate the response fields.

In the absence of body forces, the motion of a continuum is governed by the following Navier's equation in the stationary coordinate system (*OXYZ*):

$$(\lambda+\mu)\nabla_0\nabla_0\cdot\underline{\mathbf{U}}+\mu\nabla_0^2\underline{\mathbf{U}}=\rho\,\partial_t^2\underline{\mathbf{U}} \tag{6}$$

where $\nabla_0=[\,\partial_X\ \partial_Y\ \partial_Z\,]^{\mathrm{T}}$ is the Del operator, $\nabla_0^2=\partial_X^2+\partial_Y^2+\partial_Z^2$ is the Laplacian operator, $\underline{\mathbf{U}}(X,Y,Z,t)$ is the displacement vector, ρ is the density, λ and μ are the Lamé constants defined by Young's modulus E and Poisson's ratio ν.

This governing equation is first transformed to the moving coordinate system based on the relationships between the two coordinate systems, then a procedure based on the Spectral Element Method (SEM) is followed to calculate the response fields in the space–time domain related to the moving coordinate system. In this procedure, a layer spectral element and a semi-infinite spectral element are developed to respectively simulate a layer and a half-space, and the combinations of these two elements can simulate different pavement structures. It should be noted that the pavement layers are considered to be perfectly bonded in the formulation of the theoretical TSD model, while further modifications are needed to consider more realistic interface conditions. The SEM-based procedure is shown in Figure 2, which can be described as follows:

(1) The governing equation in the moving coordinate system is transformed from the space–time domain to the wavenumber-frequency domain via the forward Fourier transform;
(2) The element equilibrium equations of a layer spectral element and a semi-infinite spectral element are formulated, and they are further assembled to obtain the system equilibrium equation;
(3) The boundary conditions are applied to the system equilibrium equation to calculate the nodal displacements of the system, which are further used to calculate the response fields of a certain element;
(4) These response fields are transformed from the wavenumber-frequency domain to the space–time domain via the inverse Fourier transform.

The detailed implementation and validation of this SEM-based procedure can be found in a previous paper by authors (Sun et al., 2019). In the SEM, one element is sufficient to represent a whole layer or half-space because of the exact description of mass distribution, which feature reduces the size of the system of dynamic equations. Consequently, the computational efficiency of the theoretical TSD model is improved, which is the main advantage of the SEM-based procedure.

In this study, it is assumed that each layer of pavements consists of elastic materials that exhibit the so-called hysteretic damping, which physically means that the energy loss in a certain motion only depends on its path. This damping effect can be numerically simulated by replacing the Young's modulus E with a complex Young's modulus $\tilde{E}(k_x, \omega)$ defined in the wavenumber-frequency domain related to the moving coordinate system:

$$\tilde{E}(k_x, \omega) = E[1 + 2\mathrm{i}\xi \,\mathrm{sgn}(\omega + ck_x)] \tag{7}$$

in which ξ is the damping ratio and $\mathrm{sgn}(\cdot)$ is the signum function.

In order to simulate the loads applied by the TSD device, the loading configuration shown in Figure 3 is used in this study. Compared to previous work by authors (Sun et al., 2019; Sun et al., 2022), the loads applied by four wheel pairs are considered in this paper, which is important to obtain accurate pavement response because of the possible superposition effect of different loads. In addition, it is assumed that each wheel pair applies a constant force which is evenly distributed over two constant rectangular areas. In the moving coordinate system, the loading area is fixed. Hence, the load applied by the TSD device can be expressed as follows:

$$p_z(x, y, t) = h_0(x, y)p(t) \tag{8}$$

where $p_z(x, y, t)$ is the TSD loading function acting in the positive z-direction with dimension of force/area, $h_0(x, y)$ is the spatial distribution function of the load without dimension, and $p(t)$ is the loading history function of the load with dimension of force/area. To well represent the TSD loading configuration, the spatial distribution function can be expressed as follows:

$$h_0(x, y) = h_1(x)h_2(y) \tag{9}$$

in which $h_1(x)$ and $h_2(y)$ have the following definitions:

$$\begin{aligned} h_1(x) &= H(x_0 - |x|) + c_1 H(x_0 - |x - l_x|) \\ h_2(y) &= \left[H\left(\frac{y_0}{2} - \left|y + \frac{y_0 + d}{2}\right|\right) + H\left(\frac{y_0}{2} - \left|y - \frac{y_0 + d}{2}\right|\right)\right] \\ &\quad + c_2\left[H\left(\frac{y_0}{2} - \left|y + l_y + \frac{y_0 + d}{2}\right|\right) + H\left(\frac{y_0}{2} - \left|y + l_y - \frac{y_0 + d}{2}\right|\right)\right] \end{aligned}$$

where $H(\cdot)$ is the Heaviside step function, $2x_0$ is the length of one rectangular loading area in x-direction, y_0 is the length of one rectangular loading area in y-direction, d is the distance between two rectangular loading areas of one wheel pair, l_x is the distance between two loading axles, l_y is the length of the loading axle, c_1 and c_2 are two coefficients related to the distribution of the load. In addition, the wheel pairs of the TSD device apply constant forces on constant areas, which makes the loading history function constant, i.e. $p(t) = p_0$.

After substituting the expressions of $h_0(x, y)$ and $p(t)$ into Equation (8), the counterpart of the TSD loading function is obtained by applying the forward Fourier transform:

$$\tilde{p}_z(k_x, k_y, \omega) = \widehat{h}_1(k_x)\widehat{h}_2(k_y)\hat{p}(\omega) \tag{10}$$

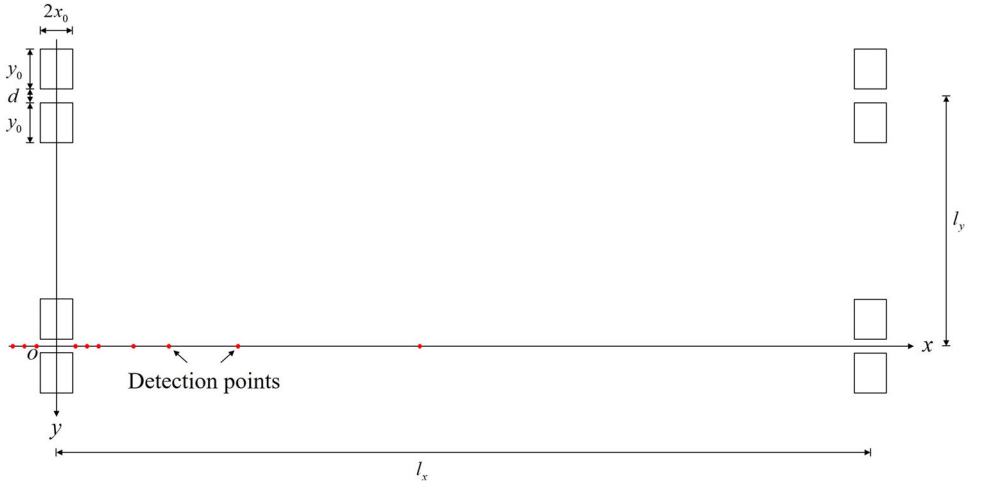

Figure 3. Loading configuration of the TSD device.

with the following definitions of $\widehat{h}_1(k_x)$, $\widehat{h}_2(k_y)$, and $\hat{p}(\omega)$:

$$\widehat{h}_1(k_x) = \begin{cases} \frac{2}{k_x}\sin(k_x x_0)\left(1 + c_1 e^{\mathrm{i}k_x l_x}\right), & k_x \neq 0 \\ 2x_0(1 + c_1), & k_x = 0 \end{cases}$$

$$\widehat{h}_2(k_y) = \begin{cases} \frac{2}{k_y}\left\{\sin\left[\frac{k_y(2y_0 + d)}{2}\right] - \sin\left(\frac{k_y d}{2}\right)\right\}\left(1 + c_2 e^{-\mathrm{i}k_y l_y}\right), & k_y \neq 0 \\ 2y_0(1 + c_2), & k_y = 0 \end{cases}$$

$$\hat{p}(\omega) = 2\pi p_0 \delta(\omega)$$

in which $\delta(\cdot)$ is the Dirac delta function.

2.2. Characteristics of model response

In this part, the characteristics of the pavement surface response caused by the whole TSD loading are investigated. According to the actual loading conditions in TSD tests, the following parameters are used to simulate the load applied by the TSD device:

- The speed of the movement $c = 13.9$m/s(50km/h);
- The magnitude of the load $p_0 = 707$kPa;
- The parameters of the loading area $c_1 = 0.6, c_2 = 1.0, l_x = 8.15$m,

  $l_y = 1.82$ m, $d = 0.15$ m, $x_0 = 0.06316$ m, and $y_0 = 0.27432$ m.

Furthermore, it is assumed that the surface response is limited in a 400 m$\times$400 m space window, the centre of which is located at the origin of the moving coordinate system. In addition, the structural parameters of the considered pavement are shown in Table 1.

For the considered pavement subjected to the whole TSD loading, the modelled vertical deflection curve and corresponding slope curve along the x-axis observed on the surface as shown in Figure 4 are obtained. These results are compared with those of a purely elastic pavement, which has the same structural parameters as the considered pavement except that all the damping ratios are zeros. The results show that, for the purely elastic pavement, the vertical deflection curve is not totally symmetric

Table 1. Structural parameters of the considered pavement.

	E	ξ	ν	ρ	h
Layers	MPa	–	–	kg/m^3	m
Surface	3000	0.05	0.3	2400	0.1
Base	500	0.05	0.3	2000	0.3
Subgrade	60	0.05	0.3	1600	Infinite

Note: E is the Young's modulus, ξ is the damping ratio, ν is the Poisson's ratio, ρ is the density, and h is the thickness.

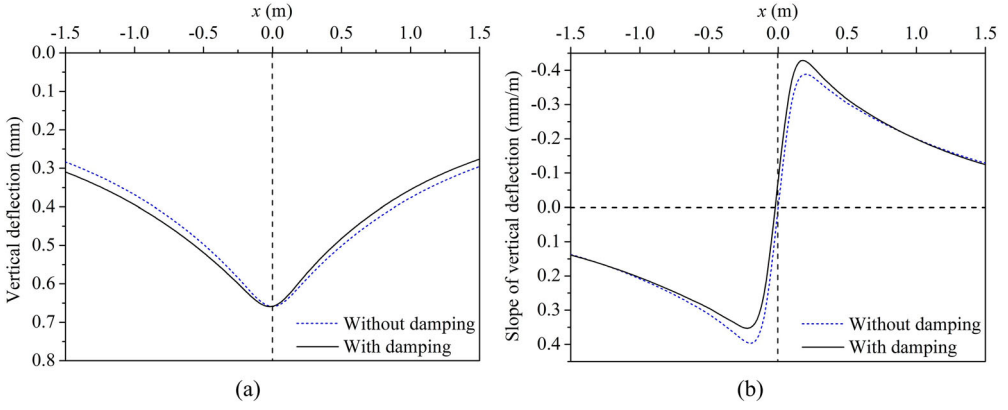

Figure 4. Comparison between the modelled response of different pavements caused by the whole TSD loading: (a) vertical deflection curve, (b) slope curve of vertical deflection.

because of the influence of the wheel pairs on the front axle and the maximum deflection appears almost at the coordinate origin; specifically, the vertical displacement of a point in front of the coordinate origin is larger than that of its symmetry point. For the pavement with hysteretic damping, the vertical deflection curve is also asymmetric and the maximum deflection appears slightly behind the coordinate origin; specifically, in the vicinity of the right rear wheel pair, the vertical displacement of a point in front of the coordinate origin is smaller than that of its symmetry point. Compared with the case of the purely elastic pavement, the vertical deflection curve of the pavement with hysteretic damping increases more slowly behind the load and decreases more quickly in front of the load with increasing x in the vicinity of the right rear wheel pair, which can also be found from the slope curves. It should be highlighted that the differences between the pavements with and without damping will be more significant if the values of the damping ratios are larger. Hence, including the damping effect is important to formulate an accurate theoretical model for the TSD test.

To have an insight into the surface deflection basin caused by the whole TSD loading, the contour curves of surface vertical deflection for the pavements with and without damping as shown in Figure 5 are obtained. The results indicate that the response at the points around the right rear wheel pair is significantly affected by the other wheel pair on the same axle, while it is slightly affected by the wheel pairs on the front axle. In addition, compared with the case of the purely elastic pavement, the TSD loading has a longer influence distance behind the device and a shorter influence distance in front of the device for the case of the pavement with hysteretic damping.

2.3. Parameter sensitivity of model response

In this part, the sensitivity of the model response to different structural parameters is investigated based on single factor analysis to have an insight into the possibility and accuracy of identifying

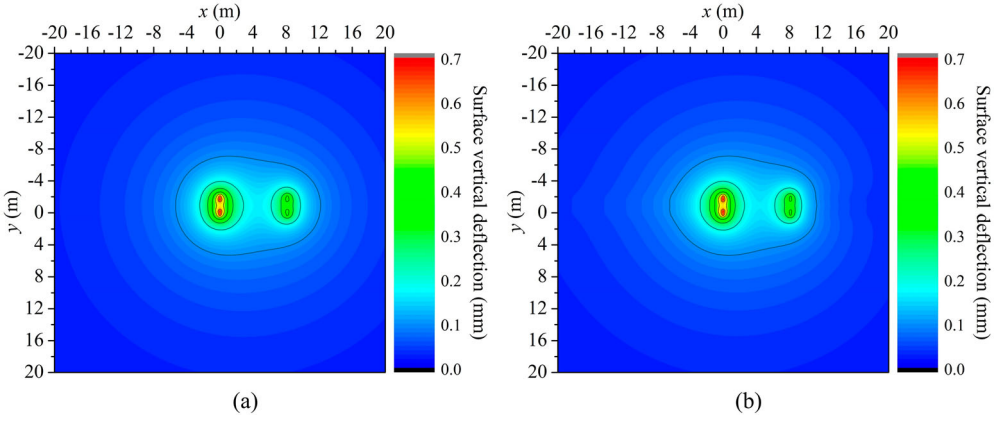

Figure 5. Contour curves of surface vertical deflection of different pavements caused by the whole TSD loading: (a) without damping, (b) with damping.

these parameters. The actual measuring conditions of TSD tests indicate that the model response of interest should be the slope curve of vertical deflection along the *x*-axis observed on a pavement surface caused by the whole TSD loading. The pavement structural parameters shown in Table 1 are considered as a reference, and the variation of a certain parameter is 50% of its reference value. The response of the reference pavement structure caused by the whole TSD loading is shown in solid lines. In addition, the subscripts '1', '2', and '3' in legends refer to the surface layer, base layer, and subgrade, respectively. For the convenience of description, the degree of sensitivity of the slope curve to different parameters is qualitatively divided into five levels: hardly sensitive, slightly sensitive, moderately sensitive, relatively sensitive, and highly sensitive.

2.3.1. Sensitivity to Young's modulus

The slope curves of pavements with different Young's moduli of the surface layer, base layer, and subgrade are shown in Figure 6(a–c), respectively. The results show that the slope curve is relatively sensitive to the Young's modulus of the surface layer, while it is highly sensitive to the Young's moduli of the base layer and subgrade.

2.3.2. Sensitivity to damping ratio

The slope curves of pavements with different damping ratios of the surface layer, base layer, and subgrade are shown in Figure 6(d–f), respectively. The results show that the slope curve is hardly sensitive to the damping ratio of the surface layer, while it is slightly sensitive to the damping ratios of the base layer and subgrade. It should be noted that the damping ratio can vary from 0 to 0.3 for different materials (Nielsen, 2019), and the slope curve could change more if the damping ratio has larger variations.

2.3.3. Sensitivity to Poisson's ratio

The slope curves of pavements with different Poisson's ratios of the surface layer, base layer, and subgrade are shown in Figure 6(g–i), respectively. The results show that the slope curve is slightly sensitive to the Poisson's ratios of the surface layer and subgrade, while it is moderately sensitive to the Poisson's ratio of the base layer.

2.3.4. Sensitivity to density

The slope curves of pavements with different densities of the surface layer, base layer, and subgrade are shown in Figure 6(j–l), respectively. The results show that the slope curve is hardly sensitive to all the densities.

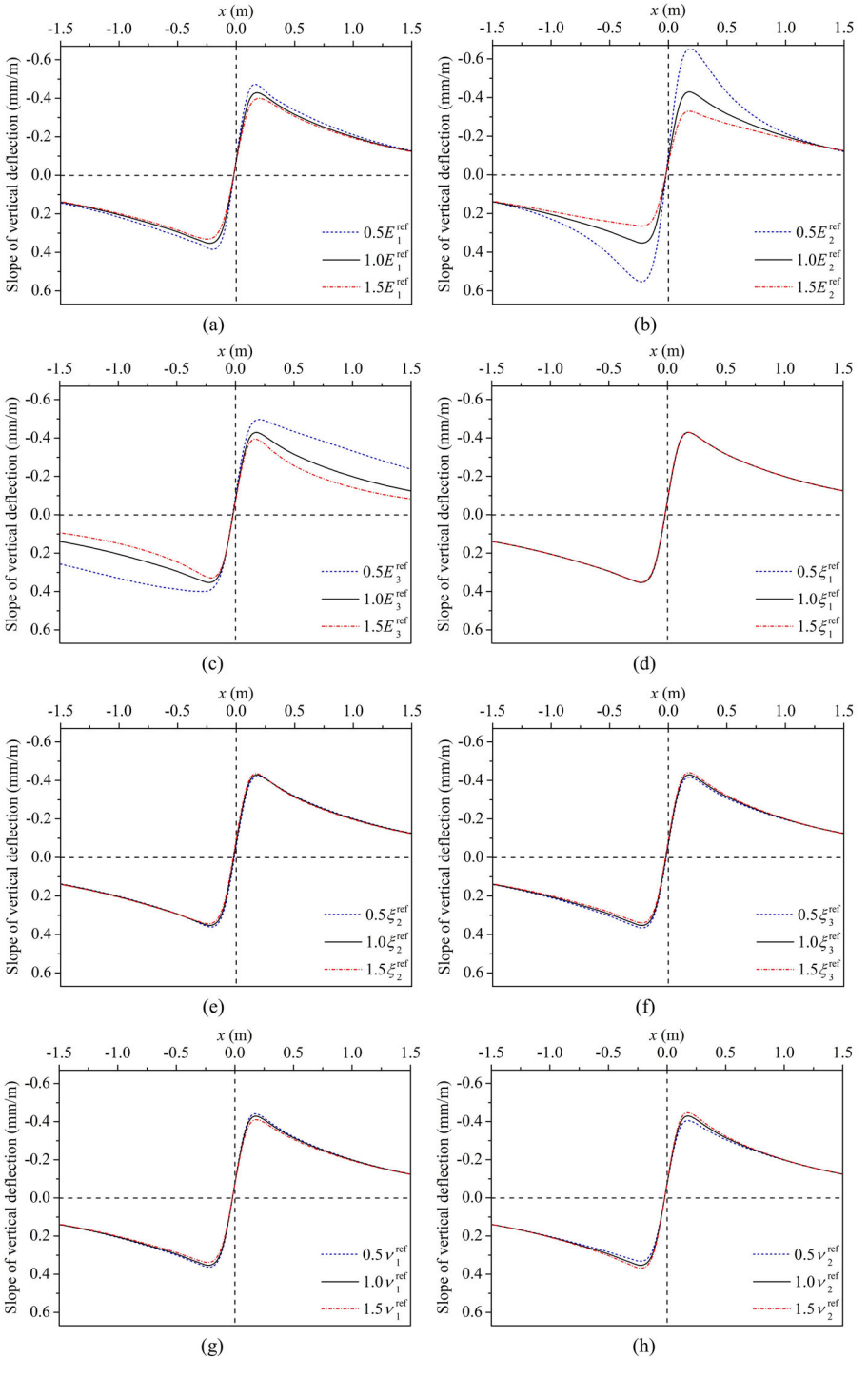

Figure 6. Sensitivity of the slope curve of vertical deflection to structural parameters: (a) Young's modulus of surface layer, (b) Young's modulus of base layer, (c) Young's modulus of subgrade, (d) Damping ratio of surface layer, (e) Damping ratio of base layer, (f) Damping ratio of subgrade, (g) Poisson's ratio of surface layer, (h) Poisson's ratio of base layer, (i) Poisson's ratio of subgrade, (j) Density of surface layer, (k) Density of base layer, (l) Density of subgrade, (m) Thickness of surface layer, (n) Thickness of base layer.

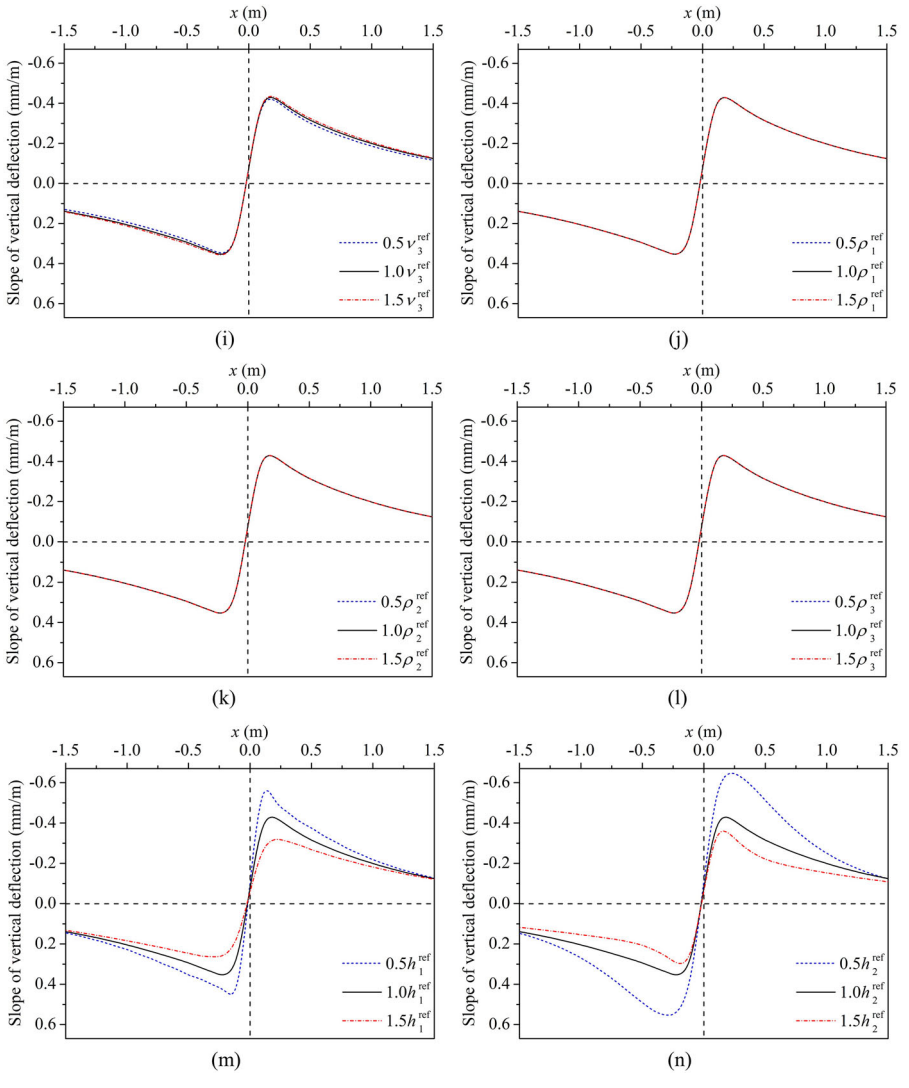

Figure 6. Continued.

2.3.5. Sensitivity to thickness

The slope curves of pavements with different thicknesses of the surface layer and base layer are shown in Figure 6(m,n), respectively. The results show that the slope curve is highly sensitive to these two thicknesses.

3. Potential minimisation algorithms

The response of a structure is determined by loading conditions and structural parameters. Theoretically, if the response and loading conditions are known, it should be possible to identify structural parameters. This process needs a so-called parameter identification technique, which can be the combination of a theoretical model and a proper minimisation algorithm. A set of most likely parameters can be found by minimising the difference between the modelled and measured response. Actually, there are many minimisation algorithms which can be used to solve multi-dimensional nonlinear equations, but a general one suitable to cope with a wide range of problems is still not available. In order to

find a minimisation algorithm which works best with the formulated theoretical model for parameter identification, three potential minimisation algorithms are considered, i.e. the factored secant update algorithm, the modified Levenberg-Marquardt algorithm, and the modified Powell hybrid algorithm. The detailed description about these three algorithms is shown below.

3.1. Factored secant update algorithm

The factored secant update algorithm can be used to solve an unconstrained system of nonlinear simultaneous equations in a manner similar to that of the Newton's method but by using a finite-difference approximation to the Jacobian. This algorithm solves a system of equations described as follows:

$$\underline{\mathbf{f}}(\underline{\mathbf{a}}) = \underline{\mathbf{0}}, \quad \text{with} \quad \underline{\mathbf{f}} : \mathbf{R}^M \rightarrow \mathbf{R}^M \quad \text{and} \quad \underline{\mathbf{a}} \in \mathbf{R}^M \tag{11}$$

where $\underline{\mathbf{f}}(\underline{\mathbf{a}})$ is the function of interest, $\underline{\mathbf{a}}$ is a vector that contains all the unknown parameters, and M is the total number of unknown parameters. In this case, the number of unknown parameters equals to the number of equations.

For a certain point $\underline{\mathbf{a}}_n$, a double dogleg method is used to approximately solve the following minimisation problem to obtain a direction vector $\underline{\mathbf{s}}_n$ at this point:

$$\min_{\underline{\mathbf{s}}_n \in \mathbf{R}^M} ||\underline{\mathbf{f}}(\underline{\mathbf{a}}_n) + \underline{\underline{\mathbf{J}}}(\underline{\mathbf{a}}_n) \cdot \underline{\mathbf{s}}_n||_2, \quad \text{subject to } ||\underline{\mathbf{s}}_n||_2 \leq \delta_n \tag{12}$$

in which $||\cdot||_2$ is the Euclidean norm, $\underline{\mathbf{f}}(\underline{\mathbf{a}}_n)$ is the function value evaluated at this point, $\underline{\underline{\mathbf{J}}}(\underline{\mathbf{a}}_n)$ is the approximate Jacobian evaluated at this point, and δ_n is the trust region which limits the size of $\underline{\mathbf{s}}_n$.

Then, the function value at the next point $\underline{\mathbf{a}}_{n+1} = \underline{\mathbf{a}}_n + \underline{\mathbf{s}}_n$ is evaluated to see whether this point should be accepted. If the point $\underline{\mathbf{a}}_{n+1}$ is rejected, the algorithm solves equation (12) again with a reduced trust region δ_n to obtain another direction vector $\underline{\mathbf{s}}_n$. This procedure is repeated until an accepted point $\underline{\mathbf{a}}_{n+1}$ is found.

If the point $\underline{\mathbf{a}}_{n+1}$ satisfies the stopping criterion, the algorithm will terminate. Otherwise, the algorithm continues from the point $\underline{\mathbf{a}}_{n+1}$ with corresponding trust region δ_{n+1} and approximate Jacobian $\underline{\underline{\mathbf{J}}}(\underline{\mathbf{a}}_{n+1})$. The approximate Jacobian $\underline{\underline{\mathbf{J}}}(\underline{\mathbf{a}}_{n+1})$ is calculated by the following Broyden's formula (Broyden, 1970):

$$\underline{\underline{\mathbf{J}}}(\underline{\mathbf{a}}_{n+1}) = \underline{\underline{\mathbf{J}}}(\underline{\mathbf{a}}_n) + \frac{[\underline{\mathbf{f}}(\underline{\mathbf{a}}_{n+1}) - \underline{\mathbf{f}}(\underline{\mathbf{a}}_n) - \underline{\underline{\mathbf{J}}}(\underline{\mathbf{a}}_n) \cdot \underline{\mathbf{s}}_n] \cdot \underline{\mathbf{s}}_n^{\mathrm{T}}}{\underline{\mathbf{s}}_n^{\mathrm{T}} \cdot \underline{\mathbf{s}}_n} \tag{13}$$

This procedure is repeated until finding a point which satisfies the stopping criterion. For more details, see the Chapter 8 in Dennis and Schnabel (1983).

3.2. Modified Levenberg-Marquardt algorithm

The modified Levenberg-Marquardt algorithm can be used to solve an unconstrained nonlinear least-squares problem by using a finite-difference approximation to the Jacobian. This algorithm combines the steepest descent method and the Newton's method. The steepest descent method is used to seek an estimate which is sufficiently close to the minimum point. Then, the Newton's method is used to refine the results until matching the stopping criterion. The nonlinear least-squares problem to be solved by this algorithm can be stated as follows:

$$\min_{\underline{\mathbf{a}} \in \mathbf{R}^N} \left[\frac{1}{2} \underline{\mathbf{f}}^{\mathrm{T}}(\underline{\mathbf{a}}) \cdot \underline{\mathbf{f}}(\underline{\mathbf{a}}) \right] = \min_{\underline{\mathbf{a}} \in \mathbf{R}^N} \left[\frac{1}{2} \sum_{m=1}^{M} f_m^2(\underline{\mathbf{a}}) \right], \quad \text{with} \quad \underline{\mathbf{f}} : \mathbf{R}^N \rightarrow \mathbf{R}^M \tag{14}$$

where $\underline{\mathbf{a}}$ is a vector that contains all the unknown parameters, $\underline{\mathbf{f}}(\underline{\mathbf{a}})$ is the function of interest, $f_m(\underline{\mathbf{a}})$ is the m-th component of the function of interest, N is the total number of unknown parameters, and

M is the total number of components of the function of interest. In addition, the relationship $M \geq N$ holds as this algorithm is suitable for solving determined/over-determined problems.

For a certain point $\underline{\mathbf{a}}_n$, the Levenberg-Marquardt algorithm modifies the Gauss–Newton algorithm by introducing a nonnegative scalar μ_n called the Levenberg-Marquardt parameter:

$$[\underline{\underline{\mathbf{J}}}^{\mathrm{T}}(\underline{\mathbf{a}}_n) \cdot \underline{\underline{\mathbf{J}}}(\underline{\mathbf{a}}_n) + \mu_n \underline{\underline{\mathbf{I}}}] \cdot \underline{\mathbf{s}}_n = -\underline{\underline{\mathbf{J}}}^{\mathrm{T}}(\underline{\mathbf{a}}_n) \cdot \underline{\mathbf{f}}(\underline{\mathbf{a}}_n) \tag{15}$$

in which $\underline{\underline{\mathbf{I}}}$ is the identity matrix of order N, $\underline{\mathbf{f}}(\underline{\mathbf{a}}_n)$ is the function value evaluated at this point, $\underline{\underline{\mathbf{J}}}(\underline{\mathbf{a}}_n)$ is the approximate Jacobian evaluated at this point, and $\underline{\mathbf{s}}_n$ is the direction vector defined by $\underline{\mathbf{s}}_n = \underline{\mathbf{a}}_{n+1} - \underline{\mathbf{a}}_n$ with $\underline{\mathbf{a}}_{n+1}$ being the next point.

By combining equation (15) and the definition of the direction vector $\underline{\mathbf{s}}_n$, the next point $\underline{\mathbf{a}}_{n+1}$ is determined as follows:

$$\underline{\mathbf{a}}_{n+1} = \underline{\mathbf{a}}_n - [\underline{\underline{\mathbf{J}}}^{\mathrm{T}}(\underline{\mathbf{a}}_n) \cdot \underline{\underline{\mathbf{J}}}(\underline{\mathbf{a}}_n) + \mu_n \underline{\underline{\mathbf{I}}}]^{-1} \cdot \underline{\underline{\mathbf{J}}}^{\mathrm{T}}(\underline{\mathbf{a}}_n) \cdot \underline{\mathbf{f}}(\underline{\mathbf{a}}_n) \tag{16}$$

If the point $\underline{\mathbf{a}}_{n+1}$ satisfies the stopping criterion, it means that the algorithm has attained the minimum successfully. Otherwise, the Levenberg-Marquardt parameter and approximate Jacobian corresponding to the point $\underline{\mathbf{a}}_{n+1}$ are submitted to equation (16) to determine the next point. This procedure is repeated until finding a point which satisfies the stopping criterion. For more details, see Levenberg (1944), Marquardt (1963), or the Chapter 10 in Dennis and Schnabel (1983).

3.3. Modified Powell hybrid algorithm

The modified Powell hybrid algorithm can be used to solve an unconstrained system of nonlinear simultaneous equations by using a finite-difference approximation to the Jacobian. The Powell hybrid algorithm requires that the number of unknown parameters should be equal to the number of equations. In addition, this algorithm determines the direction vector by using either the quasi-Newton method or the steepest descent method according to a step size criterion. For a certain point $\underline{\mathbf{a}}_n$ (a vector that contains all the unknown parameters), this algorithm first calculates the direction vector $\underline{\mathbf{s}}_n$ by using the quasi-Newton method:

$$\underline{\mathbf{s}}_n = -\underline{\underline{\mathbf{J}}}^{-1}(\underline{\mathbf{a}}_n) \cdot \underline{\mathbf{f}}(\underline{\mathbf{a}}_n) \quad \text{so that} \quad ||\underline{\mathbf{s}}_n||_2 \leq \Delta_n \tag{17}$$

where $||\cdot||_2$ is the Euclidean norm, $\underline{\mathbf{f}}(\underline{\mathbf{a}}_n)$ is the function value evaluated at this point, $\underline{\underline{\mathbf{J}}}(\underline{\mathbf{a}}_n)$ is the approximate Jacobian evaluated at this point, and Δ_n is the step size parameter.

If the criterion $||\underline{\mathbf{s}}_n||_2 \leq \Delta_n$ is satisfied, the calculated direction vector will be accepted and the next point will be determined via equation $\underline{\mathbf{a}}_{n+1} = \underline{\mathbf{a}}_n + \underline{\mathbf{s}}_n$. If this criterion fails, a second criterion will be tested:

$$\alpha_n ||\underline{\mathbf{r}}_n||_2 \geq \Delta_n \tag{18}$$

with the following definitions of α_n and $\underline{\mathbf{r}}_n$:

$$\alpha_n = \frac{\left\| \underline{\underline{\mathbf{J}}}^{\mathrm{T}}(\underline{\mathbf{a}}_n) \cdot \underline{\mathbf{f}}(\underline{\mathbf{a}}_n) \right\|_2^2}{\left\| \underline{\underline{\mathbf{J}}}(\underline{\mathbf{a}}_n) \cdot \underline{\underline{\mathbf{J}}}^{\mathrm{T}}(\underline{\mathbf{a}}_n) \cdot \underline{\mathbf{f}}(\underline{\mathbf{a}}_n) \right\|_2^2}$$

$$\underline{\mathbf{r}}_n = -\underline{\underline{\mathbf{J}}}^{\mathrm{T}}(\underline{\mathbf{a}}_n) \cdot \underline{\mathbf{f}}(\underline{\mathbf{a}}_n)$$

If this criterion is satisfied, the direction vector will be calculated by using the steepest descent method via equation $\underline{\mathbf{s}}_n = (\Delta_n / ||\underline{\mathbf{r}}_n||_2)\underline{\mathbf{r}}_n$. If the second criterion still fails, the direction vector is determined by using a hybrid between the quasi-Newton method and the steepest descent method via equation $\underline{\mathbf{s}}_n = \beta_n \underline{\mathbf{f}}(\underline{\mathbf{a}}_n) + (1 - \beta_n)\alpha_n \underline{\mathbf{r}}_n$, where β_n is chosen such that $||\underline{\mathbf{s}}_n||_2 = \Delta_n$. This procedure is repeated

until finding a point which satisfies the stopping criterion. For more details, see Scales (1985) or Moré et al. (1980).

These three minimisation algorithms are combined with the formulated theoretical model for the TSD test to achieve parameter identification based on TSD measurements. For the specific case of the TSD test, the function of interest for the minimisation process can be defined as follows:

$$f_m(\underline{\mathbf{a}}) = \left| \frac{s^{\text{modelled}}(x_m, y_m; \underline{\mathbf{a}})}{s^{\text{measured}}(x_m, y_m)} - 1 \right| \tag{19}$$

in which $f_m(\underline{\mathbf{a}})$ is the m-th component of the function of interest $\underline{\mathbf{f}}(\underline{\mathbf{a}})$, $\underline{\mathbf{a}}$ is a vector that consists of all the parameters to be identified, $s^{\text{modelled}}(x_m, y_m; \underline{\mathbf{a}})$ and $s^{\text{measured}}(x_m, y_m)$ are respectively the modelled and measured slopes of vertical deflection at detection point (x_m, y_m). It can be concluded that the smaller the value of the m-th component of the function of interest, the better the match between the modelled and measured slopes of vertical deflection at the m-th detection point. Therefore, the objective of the minimisation process is to minimise all components of the function of interest, the number of which equals to the number of detection points. In addition, the description of different minimisation algorithms indicates that the number of unknown parameters should be no more than the number of detection points. In practice, the TSD device can only measure the slopes of vertical deflection of about 9 points. Hence, some pavement parameters should be fixed to make the problem solvable.

4. Performance of different minimisation algorithms

In this section, the performance of different minimisation algorithms for parameter identification is evaluated in terms of the convergence stability and convergence rate. The convergence stability refers to the ability of an algorithm to converge to the desired minimum regardless of starting points (Scales, 1985). The convergence rate refers to the performance of an algorithm at each iteration and the total number of iterations needed for convergence.

The results of the parameter sensitivity analysis suggest that the Young's moduli and thicknesses of pavement layers are the parameters suitable for identification. However, preliminary investigation shows that the minimisation algorithms could give different combinations of Young's modulus and thickness for a given set of TSD measurements. This phenomenon is understandable because the influence caused by the change of Young's modulus can be offset by the change of thickness. According to the plate theory, the Young's modulus E and thickness h of a certain pavement layer mainly affect the response via the bending stiffness $D = Eh^3/[12(1-\nu^2)]$, where ν is the Poisson's ratio. Hence, many combinations of E and h which give the same value of Eh^3 can correspond to similar pavement response (Nielsen, 2019). In order to increase the chance to obtain unique solutions, the Young's moduli of pavement layers are chosen to be the only parameters to be identified in this study.

In what follows, some case studies are conducted to evaluate the performance of different minimisation algorithms for parameter identification by processing synthetic TSD measurements. It should be highlighted that all the presented case studies are conducted on a midrange laptop with a quad-core i7-7700HQ CPU. For a certain minimisation algorithm, the performance of the computer used can affect the computational time, but it does not affect the number of iterations needed to converge. Hence, the number of iterations is an important parameter for characterising the performance of minimisation algorithms.

4.1. Parameter identification of a typical pavement

A pavement with structural parameters shown in Table 1 is considered as a typical pavement, and the modelled vertical deflection slopes of three points ($x = -0.269$, 0.163, and 0.362 m) along the x-axis on the pavement surface caused by the whole TSD loading are taken as the synthetic TSD measurements.

Table 2. Cases with different initial guesses for the typical pavement.

	E_1	E_2	E_3
Cases	MPa	MPa	MPa
1	3500	600	70
2	2500	400	50
3	2500	600	70
4	3500	400	70
5	3500	600	50
6	2500	400	70
7	2500	600	50
8	3500	400	50

These synthetic measurements are analysed by parameter identification techniques using different minimisation algorithms to determine the Young's moduli of pavement layers, the true values of which are $E_1 = 3000$ MPa, $E_2 = 500$ MPa, and $E_3 = 60$ MPa.

The function of interest for the minimisation process depends nonlinearly on the unknown parameter vector. Hence, for different initial guesses, the proposed technique could give different parameter vectors corresponding to different minima. In addition, the convergence rate relates to the computational efficiency of the proposed technique. Hence, it is meaningful to investigate both the convergence stability and convergence rate of the proposed technique. Preliminary investigation shows that good initial guesses of unknown parameters are important to the parameter identification process. Therefore, some auxiliary tools could be used to find a good set of initial guesses. In order to conduct a comprehensive study on the convergence stability and convergence rate of the proposed technique, eight cases with different initial guesses shown in Table 2 are considered. These cases are generated by considering that each parameter has two initial guesses, and the variation of the initial guesses is about 15% of the corresponding true value. This principle is consistently used to generate cases with different initial guesses.

The quality of the results of the parameter identification can be evaluated by the error between the identified values and true values, which can be quantified by a dimensionless quantity ε_p defined as follows:

$$\varepsilon_p = \sqrt{\frac{1}{N}\sum_{n=1}^{N}\left(\frac{a_n^{\text{identified}}}{a_n^{\text{true}}} - 1\right)^2} \tag{20}$$

where $a_n^{\text{identified}}$ is the n-th component of the identified parameter vector $\underline{\mathbf{a}}^{\text{identified}}$, a_n^{true} is the n-th component of the true parameter vector $\underline{\mathbf{a}}^{\text{true}}$, and N is the total number of the parameters to be identified. It can be concluded that a minimisation algorithm converges to the true parameter values if the quantity ε_p of the identified parameter values is small. For all the cases with different initial guesses considered by a minimisation algorithm, the percentage of cases that converge to the true parameter values is used to evaluate the convergence stability of the algorithm; the average number of iterations needed to converge is used to evaluate the convergence rate of the algorithm. The results obtained by different minimisation algorithms are presented below.

4.1.1. Factored secant update algorithm

The results obtained by the factored secant update algorithm for the typical pavement are shown in Table 3. The results show that all the cases converge to the true parameter values, hence the factored secant update algorithm has good convergence stability to identify the parameters of the typical pavement if a good set of initial guesses is provided. In addition, the average number of iterations in the parameter identification process is about 68 (each iteration takes about 2 min), which indicates that the convergence rate of this algorithm is not that high when compared to the other algorithms.

Table 3. Results obtained by the factored secant update algorithm for the typical pavement.

	E_1	E_2	E_3	ϵ_p	Iterations
Cases	MPa	MPa	MPa	–	–
1	3000.000	500.000	60.000	1.4E-08	82
2	3000.000	500.000	60.000	4.6E-10	47
3	3000.000	500.000	60.000	9.2E-09	88
4	3000.065	500.019	59.994	6.6E-05	80
5	3000.000	500.000	60.000	4.9E-10	48
6	3000.000	500.000	60.000	5.3E-10	67
7	3000.000	500.000	60.000	1.8E-09	50
8	3000.019	500.000	60.000	3.9E-06	80

Table 4. Results obtained by the modified Levenberg-Marquardt algorithm for the typical pavement (3 detection points).

	E_1	E_2	E_3	ϵ_p	Iterations
Cases	MPa	MPa	MPa	–	–
1	2999.995	500.000	60.000	1.0E-06	17
2	3000.236	499.986	60.002	5.1E-05	17
3	2999.914	500.005	59.999	1.9E-05	17
4	2999.988	500.001	60.000	2.7E-06	17
5	2999.997	500.000	60.000	5.7E-07	17
6	3000.016	499.999	60.000	3.6E-06	17
7	3000.009	499.999	60.000	2.1E-06	17
8	3000.043	499.997	60.000	9.6E-06	17

Hence, the corresponding parameter identification technique is not that computationally efficient to deal with TSD measurements obtained from network-level testing.

4.1.2. Modified Levenberg-Marquardt algorithm

If the vertical deflection slopes of only the three detection points are used for parameter identification, the results obtained by the modified Levenberg-Marquardt algorithm for the typical pavement are shown in Table 4. The results indicate that all the cases converge to the true parameter values, hence the modified Levenberg-Marquardt algorithm has good convergence stability to identify the parameters of the typical pavement if a good set of initial guesses is provided. In addition, the average number of iterations in the parameter identification process is 17 (each iteration takes about 2 min), which indicates that this algorithm has high convergence rate. Hence, the corresponding parameter identification technique has high computational efficiency to deal with TSD measurements obtained from network-level testing.

In addition, the modified Levenberg-Marquardt algorithm has the ability to solve over-determined systems. Hence, in order to make full use of the TSD measurements, the vertical deflection slopes of all the nine detection points ($x = -0.366$, -0.269, -0.167, 0.163, 0.260, 0.362, 0.662, 0.964, and 1.559 m) along the x-axis on the pavement surface are used for parameter identification. With using nine detection points, the results obtained by the modified Levenberg-Marquardt algorithm for the typical pavement are shown in Table 5. It can be seen that all the cases also converge to the true parameter values after about 17 iterations (each iteration takes about 2 min). There is no obvious difference between using three detection points and using nine detection points for identifying layer moduli of the typical pavement.

4.1.3. Modified Powell hybrid algorithm

The results obtained by the modified Powell hybrid algorithm for the typical pavement are shown in Table 6. The results show that all the cases converge to the true parameter values, hence the modified Powell hybrid algorithm also has good convergence stability to identify the parameters of the typical

Table 5. Results obtained by the modified Levenberg-Marquardt algorithm for the typical pavement (9 detection points).

	E_1	E_2	E_3	ϵ_p	Iterations
Cases	MPa	MPa	MPa	–	–
1	3000.000	500.000	60.000	1.2E-08	17
2	3000.000	500.000	60.000	1.8E-08	17
3	3000.000	500.000	60.000	6.3E-08	17
4	3000.000	500.000	60.000	1.1E-07	17
5	2999.784	500.015	59.998	4.9E-05	13
6	3000.000	500.000	60.000	2.4E-09	17
7	2999.999	500.000	60.000	1.3E-07	17
8	3000.001	500.000	60.000	2.6E-07	17

Table 6. Results obtained by the modified Powell hybrid algorithm for the typical pavement.

	E_1	E_2	E_3	ϵ_p	Iterations
Cases	MPa	MPa	MPa	–	–
1	3000.000	500.000	60.000	5.7E-08	28
2	3000.026	499.957	60.003	5.8E-05	13
3	2995.012	500.590	59.932	1.3E-03	28
4	3000.012	499.999	60.000	2.5E-06	26
5	3000.301	499.655	60.028	4.8E-04	21
6	3000.008	500.000	59.998	1.9E-05	19
7	2999.994	500.001	60.000	1.9E-06	22
8	2999.868	500.001	59.999	2.8E-05	20

Table 7. Structural parameters of the pavement with rigid base.

	E	ξ	ν	ρ	h
Layers	MPa	–	–	kg/m^3	m
Surface	3000	0.05	0.3	2400	0.1
Base	5000	0.05	0.3	2000	0.3
Subgrade	60	0.05	0.3	1600	Infinite

Note: E is the Young's modulus, ξ is the damping ratio, ν is the Poisson's ratio, ρ is the density, and h is the thickness.

pavement if a good set of initial guesses is provided. In addition, the average number of iterations in the parameter identification process is about 22 (each iteration takes about 2 min), which indicates that the convergence rate of this algorithm is relatively high. Hence, the corresponding parameter identification technique has relatively high computational efficiency to deal with TSD measurements obtained from network-level testing.

4.2. Parameter identification of a pavement with rigid base

In this part, the performance of different minimisation algorithms in identifying parameters of a pavement with rigid base is investigated. The reason for considering this type of pavement is that using a stiff base layer is necessary in engineering practice if the subgrade is composed of a kind of weak soil. In addition, parameter identification techniques may exhibit numerical instability when dealing with the response of this type of pavement (Al-Khoury, 2002). The structural parameters of the considered pavement are shown in Table 7, which implies that the Young's modulus of the base layer is relatively high. For this pavement, the modelled vertical deflection slopes of three points ($x = -0.269$, 0.163, and 0.362 m) along the x-axis on the pavement surface caused by the whole TSD loading are taken as the synthetic TSD measurements. These synthetic measurements are analysed by the proposed technique to identify the Young's moduli of pavement layers.

Table 8. Cases with different initial guesses for the pavement with rigid base.

	E_1	E_2	E_3
Cases	MPa	MPa	MPa
1	3500	6000	70
2	2500	4000	50
3	2500	6000	70
4	3500	4000	70
5	3500	6000	50
6	2500	4000	70
7	2500	6000	50
8	3500	4000	50

Table 9. Results obtained by the factored secant update algorithm for the pavement with rigid base.

	E_1	E_2	E_3	ϵ_p	Iterations
Cases	MPa	MPa	MPa	–	–
1	3000.000	5000.000	60.000	4.2E-08	77
2	3000.000	5000.000	60.000	2.4E-08	71
3	3000.000	5000.000	60.000	1.5E-08	157
4	3000.000	5000.000	60.000	8.1E-08	87
5	3000.000	5000.000	60.000	8.5E-08	131
6	3000.005	4999.998	60.000	1.7E-06	152
7	3000.000	5000.000	60.000	3.8E-08	214
8	2996.198	5000.496	60.038	8.2E-04	244

In order to investigate the convergence stability and convergence rate of different minimisation algorithms to identify parameters of the pavement with rigid base, eight cases with different initial guesses shown in Table 8 are considered. The results obtained by different minimisation algorithms are presented below.

4.2.1. Factored secant update algorithm

The results obtained by the factored secant update algorithm for the pavement with rigid base are shown in Table 9. It can be seen that all the cases converge to the true parameter values, hence the factored secant update algorithm has good convergence stability to identify the parameters of the pavement with rigid base if a good set of initial guesses is provided. In addition, the average number of iterations is about 142, which indicates that the convergence rate of this algorithm is not that high either for the case of a pavement with rigid base.

4.2.2. Modified Levenberg-Marquardt algorithm

If the vertical deflection slopes of only the three detection points are used for parameter identification, the results obtained by the modified Levenberg-Marquardt algorithm for the pavement with rigid base are shown in Table 10. It can be seen that only cases 5 and 7 converge to the true parameter values, while the other cases converge to combinations of other parameter values which correspond to other local minima. Hence, the convergence stability of the modified Levenberg-Marquardt algorithm to identify the parameters of the pavement with rigid base is not that good when considering three detection points, although the convergence rate of this algorithm is relatively high (the average number of iterations is about 30).

In addition, the performance of the modified Levenberg-Marquardt algorithm with considering all the nine detection points is also investigated. When the modelled vertical deflection slopes of the nine detection points ($x = -0.366, -0.269, -0.167, 0.163, 0.260, 0.362, 0.662, 0.964$, and 1.559 m) along the x-axis on the pavement surface are used for parameter identification, the results shown in Table 11 are obtained. It can be seen that all the cases converge to the true parameter values, hence the modified Levenberg-Marquardt algorithm has good convergence stability to identify the parameters of the

Table 10. Results obtained by the modified Levenberg-Marquardt algorithm for the pavement with rigid base (3 detection points).

	E_1	E_2	E_3	ϵ_p	Iterations
Cases	MPa	MPa	MPa	–	–
1	4064.404	4887.350	50.207	2.3E-01	24
2	1636.563	5106.498	80.687	3.3E-01	26
3	3789.190	4912.795	52.510	1.7E-01	32
4	3895.932	4905.666	51.533	1.9E-01	28
5	2993.480	5000.625	60.074	1.4E-03	32
6	1636.414	5106.503	80.690	3.3E-01	29
7	2995.834	5000.400	60.047	9.2E-04	37
8	3660.327	4931.686	53.463	1.4E-01	35

Table 11. Results obtained by the modified Levenberg-Marquardt algorithm for the pavement with rigid base (9 detection points).

	E_1	E_2	E_3	ϵ_p	Iterations
Cases	MPa	MPa	MPa	–	–
1	2999.986	5000.002	60.000	3.7E-06	17
2	2999.984	5000.008	60.000	3.2E-06	17
3	2999.998	5000.002	60.000	4.1E-07	17
4	2999.998	5000.002	60.000	5.0E-07	17
5	3000.013	4999.998	60.000	2.8E-06	21
6	2999.959	5000.021	60.000	8.3E-06	17
7	3000.055	5000.004	59.999	1.3E-05	17
8	2999.980	5000.016	60.000	4.3E-06	17

Table 12. Results obtained by the modified Powell hybrid algorithm for the pavement with rigid base.

	E_1	E_2	E_3	ϵ_p	Iterations
Cases	MPa	MPa	MPa	–	–
1	2999.998	5000.000	60.000	4.5E-07	83
2	1636.452	5106.502	80.689	3.3E-01	39
3	2999.712	5000.026	60.003	6.1E-05	53
4	2999.940	5000.006	60.001	1.3E-05	91
5	2999.992	5000.001	60.000	1.7E-06	73
6	3000.198	4999.981	59.998	4.4E-05	52
7	3004.719	4999.547	59.946	1.0E-03	56
8	3000.464	4999.959	59.995	1.0E-04	94

pavement with rigid base when considering all the nine detection points. In addition, the average number of iterations is about 18, which indicates that the convergence rate of this algorithm is also high when considering all the nine detection points.

4.2.3. Modified Powell hybrid algorithm

The results obtained by the modified Powell hybrid algorithm for the pavement with rigid base are shown in Table 12. It can be seen that most cases converge to the true parameter values except case 2, which converges to a combination of other parameter values corresponding to a local minimum. Hence, the convergence stability of the modified Powell hybrid algorithm to identify the parameters of the pavement with rigid base is relatively good. In addition, the average number of iterations needed to converge is about 68, which indicates that the convergence rate of this algorithm is not that high when analysing the response of the pavement with rigid base.

It is worth noting that case 2 can converge to true parameter values if the initial guesses have less variations. For example, if the initial guesses in case 2 are chosen to be $E_1 = 2500$ MPa,

Table 13. Performance of different minimisation algorithms for parameter identification.

	Typical pavement		Pavement with rigid base	
Algorithms	Accuracy	Iterations	Accuracy	Iterations
Secant	100%	68	100%	142
LM-3	100%	17	25%	30
LM-9	100%	17	100%	18
Powell	100%	22	87.5%	68

$E_2 = 4500$ MPa, and $E_3 = 50$ MPa, the following parameter values are identified after 73 iterations: $E_1 = 3000.001$ MPa, $E_2 = 5000.000$ MPa, and $E_3 = 60.000$ MPa. These identified parameter values are very close to the true parameter values.

4.3. Performance comparison

On the basis of the results presented above, the performance of different minimisation algorithms for parameter identification is summarised in Table 13. In this table, 'Secant' represents the factored secant update algorithm, 'LM-3' represents the modified Levenberg-Marquardt algorithm using 3 detection points, 'LM-9' represents the modified Levenberg-Marquardt algorithm using all the 9 detection points, and 'Powell' represents the modified Powell hybrid algorithm. This table shows that analysing the response of the pavement with rigid base generally has lower accuracy and needs more iterations to converge than analysing the response of the typical pavement. Compared with other algorithms, the LM-9 has the highest overall performance for parameter identification, it takes about 35 min to conduct an accurate parameter identification on a laptop with average performance. Hence, in what follows, the modified Levenberg-Marquardt algorithm using all the 9 detection points will be combined with the theoretical model to achieve parameter identification.

5. Performance in processing field TSD measurements

In practice, the TSD measurements will contain a certain degree of error introduced by the measuring system or external environment. Hence, it is important to investigate the performance of the developed technique in processing field data. The field TSD measurements used in this section are derived from the measurements at a location 5.17 km on a road section near Copenhagen, as presented in the literature by Nielsen (2019). In the parameter identification process, the whole TSD loading is represented by the following parameters:

- The speed of the movement $c = 22.2$m/s(80km/h);
- The magnitude of the load $p_0 = 707$kPa;
- The parameters of the loading area $c_1 = 0.6, c_2 = 1.0, l_x = 8.15$m,

  $l_y = 1.82$ m, $d = 0.15$ m, $x_0 = 0.06316$ m, and $y_0 = 0.27432$ m.

In addition, the dimension of the space window is 400 m$\times$400 m. In what follows, the combination of the theoretical model and the modified Levenberg-Marquardt algorithm using all the 9 detection points (LM-9) is used to process field TSD measurements for parameter identification.

5.1. Performance in identifying layer moduli

In this part, the performance of the developed technique in identifying layer moduli of pavements based on field TSD measurements is investigated. The other structural parameters of pavements are assumed to have values shown in Table 14.

Table 14. The values of other structural parameters.

	ξ	ν	ρ	h
Layers	–	–	kg/m^3	m
Surface	0.25	0.3	2400	0.1
Base	0.15	0.3	2000	0.3
Subgrade	0.10	0.3	1600	Infinite

Note: ξ is the damping ratio, ν is the Poisson's ratio, ρ is the density, and h is the thickness.

Table 15. Initial guesses and identified values of layer moduli.

	Initial guesses (MPa)			Identified values (MPa)			Iterations
Cases	E_1	E_2	E_3	E_1	E_2	E_3	–
1	700	20	10	3517.2	123.4	56.9	29
2	1000	100	10	3518.1	123.3	56.9	29
3	5000	500	50	3517.0	123.4	56.9	26
4	6000	200	50	3516.0	123.4	56.9	22
5	6000	200	100	3505.6	123.7	56.9	26

In the process of parameter identification, 5 cases with different initial guesses shown in Table 15 are considered. The identified values of layer moduli and number of iterations needed for convergence are also shown in Table 15. It can be seen that the identified values of layer moduli are almost identical for different cases, which confirms the good convergence stability of this technique. Furthermore, the comparison between case 4 and case 5 shows that a larger deviation between the initial guess and the right solution results in more iterations to converge. In general, more iterations are needed to converge and/or less accurate parameter values are obtained if the initial guess has a larger deviation from the right solution. It should be highlighted that the technique used can converge to an incorrect solution if the initial guess is not that good. For example, if the initial guess is chosen to be: $E_1 = 100$ MPa, $E_2 = 100$ MPa, and $E_3 = 10$ MPa, the following parameter values are identified after 25 iterations: $E_1 = 98.0$ MPa, $E_2 = 272.3$ MPa, and $E_3 = 59.9$ MPa. Hence, a good set of initial guesses is important for the parameter identification technique to converge to the right solution. In addition, the average number of iterations for the considered cases is about 26 (each iteration takes about 2 min), which indicates that this technique has relatively high convergence rate to process field TSD measurements.

To check the validity of the identified parameter values, the modelled vertical deflection slope curve corresponding to the parameter values identified in case 4 is compared with the measurements, as shown in Figure 7. The good match between the modelled and measured data confirms the validity of the identified parameter values. Hence, the combination of the theoretical model and the LM-9 can be used to identify layer moduli of pavements on the basis of field TSD measurements.

However, due to the nature of multiple solutions in the parameter identification of layered systems, the identified layer moduli are only reliable when the other parameters (especially the layer thicknesses) are reliable. For example, when the thickness of the surface layer in Table 14 is assumed to be 0.2 m and all the other parameters remain unchanged, the layer moduli shown in Table 16 are identified for cases with different initial guesses. It can be seen that this technique stably converges to the same solution for the identification of layer moduli. Furthermore, compared with the identified layer moduli when assuming h_1 to be 0.1 m, the identified E_1 is significantly smaller and the identified E_2 is relatively smaller when assuming h_1 to be 0.2 m. Hence, to ensure the validity of the identified parameters, the parameters which are not intended to be identified should be close to reality, especially the parameters that have significant influence on the response (such as the layer thicknesses). To accurately determine the layer thicknesses of pavements, the Ground Penetrating Radar (GPR) is recommended to be used.

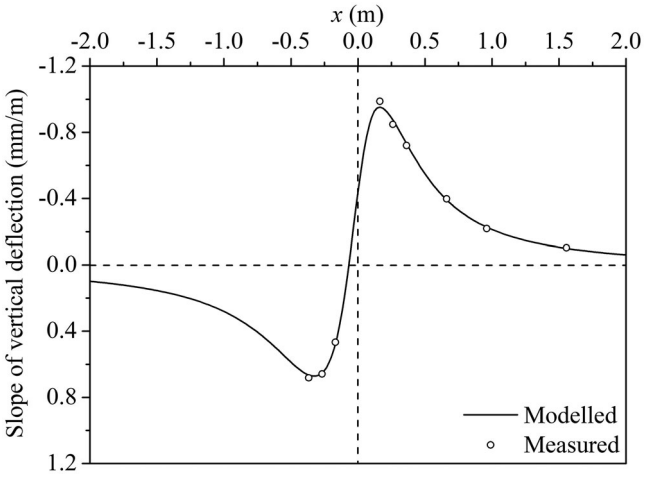

Figure 7. Comparison between modelled and measured data.

Table 16. Results of parameter identification when the thickness of the surface layer is assumed to be 0.2 m.

	Initial guesses (MPa)			Identified values (MPa)			Iterations
Cases	E_1	E_2	E_3	E_1	E_2	E_3	–
1	100	10	10	612.1	85.9	58.0	29
2	1000	100	100	612.0	85.9	58.0	22
3	3000	200	50	612.0	85.9	58.0	22
4	6000	200	50	612.1	85.9	58.0	35
5	5000	500	500	612.1	85.9	58.0	45

Table 17. Cases with different initial guesses for the identification of layer moduli and damping ratios.

	E_1	E_2	E_3	ξ_1	ξ_2	ξ_3
Cases	MPa	MPa	MPa	–	–	–
1	700	20	10	0.05	0.05	0.05
2	1000	100	10	0.10	0.10	0.10
3	5000	500	50	0.15	0.15	0.15
4	6000	200	50	0.20	0.20	0.20
5	6000	200	100	0.25	0.25	0.25

5.2. Performance in identifying layer moduli and damping ratios

In this part, the performance of the developed technique in identifying layer moduli and damping ratios of pavements based on field TSD measurements is investigated. The other structural parameters of pavements are maintained to be the same as those shown in Table 14. In the parameter identification process, 5 cases with different initial guesses shown in Table 17 are considered. The corresponding identified parameter values are shown in Table 18. It can be seen that all the cases converge to almost the same solution, which confirms the good convergence stability of the developed technique. In addition, the average number of iterations for convergence is about 54 (each iteration takes about 2 min), which indicates that the identification of layer moduli and damping ratios at the same time is not that computationally efficient.

6. Conclusions and recommendations

This paper formulates a theoretical model for the Traffic Speed Deflectometer (TSD) test, based on which the characteristics and parameter sensitivity of the pavement response caused by the whole TSD

Table 18. Results of the identification of layer moduli and damping ratios.

	E_1	E_2	E_3	ξ_1	ξ_2	ξ_3	Iterations
Cases	MPa	MPa	MPa	–	–	–	–
1	3176.5	123.4	56.4	0.307	0.169	0.087	57
2	3219.4	122.6	56.4	0.301	0.172	0.085	50
3	3176.2	123.4	56.4	0.307	0.169	0.087	60
4	3194.6	123.0	56.4	0.304	0.171	0.086	37
5	3228.5	122.4	56.4	0.298	0.173	0.084	65

loading are investigated. Furthermore, this theoretical model is combined with different minimisation algorithms for the purpose of parameter identification. The minimisation algorithm with the best performance is selected after comparison, and its performance in processing field TSD measurements is investigated. According to the results and discussions presented above, the following conclusions can be drawn:

- The developed theoretical model for the TSD test can accurately capture the effect of hysteretic damping on the response of pavements caused by moving loads, which is important to ensure the accuracy of the parameter identification based on TSD measurements.
- After comparison, the modified Levenberg-Marquardt algorithm using all the 9 detection points (LM-9) is suggested to be combined with the theoretical TSD model for the purpose of parameter identification.
- On a laptop with average performance, the proposed technique needs about 50 min to accurately identify layer moduli of pavements based on TSD measurements, so it is a promising parameter identification technique for the TSD test of pavements.

In future work, the performance of the proposed parameter identification technique in dealing with a large number of field TSD measurements is recommended to be investigated.

Acknowledgements

The first author is grateful for the financial support of the China Scholarship Council.

Disclosure statement

No potential conflict of interest was reported by the author(s).

Funding

This work was supported by the China Scholarship Council [grant number: 201608230114].

ORCID

Zhaojie Sun http://orcid.org/0000-0002-4219-1816
Cor Kasbergen http://orcid.org/0000-0002-7076-2348
Karel N. van Dalen http://orcid.org/0000-0002-8552-1811
Kumar Anupam http://orcid.org/0000-0003-4033-637X
Athanasios Skarpas http://orcid.org/0000-0001-9146-1600
Sandra M. J. G. Erkens http://orcid.org/0000-0002-2465-7643

References

Al-Khoury, R. (2002). *Parameter identification technique for layered systems* [PhD dissertation]. Delft University of Technology, The Netherlands.

Al-Khoury, R., Kasbergen, C., Scarpas, A., & Blaauwendraad, J. (2001b). Spectral element technique for efficient parameter identification of layered media. Part II: Inverse calculation. *International Journal of Solids and Structures*, *38*(48-49), 8753–8772. https://doi.org/10.1016/S0020-7683(01)00109-3

Al-Khoury, R., Scarpas, A., Kasbergen, C., & Blaauwendraad, J. (2001a). Spectral element technique for efficient parameter identification of layered media. Part I: Forward calculation. *International Journal of Solids and Structures*, *38*(9), 1605–1623. https://doi.org/10.1016/S0020-7683(00)00112-8

Broyden, C. G. (1970). The convergence of a class of double-rank minimization algorithms: General considerations. *IMA Journal of Applied Mathematics*, *6*(1), 76–90.

Dennis, J. E., Jr., & Schnabel, R. B. (1983). *Numerical methods for unconstrained optimization and nonlinear equations*. Prentice-Hall.

Katicha, S. W., Flintsch, G., Bryce, J., & Ferne, B. (2014). Wavelet denoising of TSD deflection slope measurements for improved pavement structural evaluation. *Computer-Aided Civil and Infrastructure Engineering*, *29*(6), 399–415. https://doi.org/10.1111/mice.12052

Kutay, M. E., Chatti, K., & Lei, L. (2011). Backcalculation of dynamic modulus mastercurve from falling weight deflectometer surface deflections. *Transportation Research Record: Journal of the Transportation Research Board*, *2227*(1), 87–96. https://doi.org/10.3141/2227-10

Lee, H. S., Ayyala, D., & Von Quintus, H. (2017). Dynamic backcalculation of viscoelastic asphalt properties and master curve construction. *Transportation Research Record: Journal of the Transportation Research Board*, *2641*(1), 29–38. https://doi.org/10.3141/2641-05

Lee, H. S., Steele, D., & Von Quintus, H. (2019). Who says backcalculation is only about layer moduli? *Transportation Research Record: Journal of the Transportation Research Board*, *2673*(1), 317–331. https://doi.org/10.1177/0361198118821337

Levenberg, K. (1944). A method for the solution of certain non-linear problems in least squares. *Quarterly of Applied Mathematics*, *2*(2), 164–168. https://doi.org/10.1090/qam/10666

Liu, P., Wang, D., Otto, F., Hu, J., & Oeser, M. (2018). Application of semi-analytical finite element method to evaluate asphalt pavement bearing capacity. *International Journal of Pavement Engineering*, *19*(6), 479–488. https://doi.org/10.1080/10298436.2016.1175562

Marquardt, D. W. (1963). An algorithm for least-squares estimation of nonlinear parameters. *Journal of the Society for Industrial and Applied Mathematics*, *11*(2), 431–441. https://doi.org/10.1137/0111030

Maser, K. R. (2003). *Non-destructive measurement of pavement layer thickness* (Report No. FHWA/CA/OR-2003/03, Contract No. 65A0074). California Department of Transportation.

Moré, J. J., Garbow, B. S., & Hillstrom, K. E. (1980). *User guide for MINPACK-1* (Report No. ANL-80-74). Argonne National Labs, Argonne, IL.

Nasimifar, M., Thyagarajan, S., Chaudhari, S., & Sivaneswaran, N. (2019). Pavement structural capacity from traffic speed deflectometer for network level pavement management system application. *Transportation Research Record: Journal of the Transportation Research Board*, *2673*(2), 456–465. https://doi.org/10.1177/0361198118825122

Nasimifar, M., Thyagarajan, S., & Sivaneswaran, N. (2017). Back-calculation of flexible pavement layer moduli from traffic speed deflectometer data. *Transportation Research Record: Journal of the Transportation Research Board*, *2641*(1), 66–74. https://doi.org/10.3141/2641-09

Nielsen, C. P. (2019). Visco-elastic back-calculation of traffic speed deflectometer measurements. *Transportation Research Record: Journal of the Transportation Research Board*, *2673*(12), 439–448. https://doi.org/10.1177/0361198118823500

Scales, L. E. (1985). *Introduction to non-linear optimization*. Macmillan.

Sun, Z., Kasbergen, C., Skarpas, A., Anupam, K., van Dalen, K. N., & Erkens, S. M. J. G. (2019). Dynamic analysis of layered systems under a moving harmonic rectangular load based on the spectral element method. *International Journal of Solids and Structures*, *180-181*, 45–61. https://doi.org/10.1016/j.ijsolstr.2019.06.022

Sun, Z., Kasbergen, C., Skarpas, A., van Dalen, K. N., Anupam, K., & Erkens, S. M. J. G. (2022). A nonlinear spectral element model for the simulation of traffic speed deflectometer tests of asphalt pavements. *International Journal of Pavement Engineering*, *23*(4), 1186–1197. https://doi.org/10.1080/10298436.2020.1795170

Sun, Z., Kasbergen, C., van Dalen, K. N., Anupam, K., Erkens, S. M. J. G., & Skarpas, A. (2020b). A parameter back-calculation technique for pavements under moving loads. In *Contributions to the 2nd International Conference on Advances in Materials and Pavement Performance Prediction-AM3P 2020* (pp. 236–240). CRC Press.

Sun, Z., Kasbergen, C., van Dalen, K. N., Anupam, K., Skarpas, A., & Erkens, S. M. J. G. (2020a). Parameter identification of asphalt pavements subjected to moving loads. In *Proceedings of the 9th International Conference on Maintenance and Rehabilitation of Pavements-Mairepav9* (pp. 785–794). Springer, Cham.

Wu, C., Wang, H., Zhao, J., Jiang, X., & Qiu, Y. (2020). Asphalt pavement modulus backcalculation using surface deflections under moving loads. *Computer-Aided Civil and Infrastructure Engineering*, *35*(11), 1246–1260. https://doi.org/10.1111/mice.12624

Zihan, Z. U. A., Elseifi, M. A., Gaspard, K., & Zhang, Z. (2019). Relationship between surface-measured indices and in-service pavement structural conditions predicted from traffic speed deflection devices. *Transportation Research Record: Journal of the Transportation Research Board*, *2673*(2), 593–604. https://doi.org/10.1177/0361198119827575